1. Introduction

Diode lasers have turned into a ubiquitous component used in a wide range of modern-day applications. This is due to a number of desirable properties, including low cost per emitted power, high electrical-to-optical conversion efficiency, small footprint, wavelength versatility, and long lifetimes. They are applied in, for instance, fiber-based optical communication systems, in chemical and ranging sensors, medical apparatus, e.g. for surgery, as well as in industrial tools for materials processing [Bac07].
As one prominent diode-laser representative, this thesis studies GaAs-based high-power broad-area laser bars emitting in the 9xx nm wavelength range. Such bars typically come as 1 cm-wide chips, have several individual diode lasers (emitters) processed onto them, and thereby upscale the total emitted power to between several hundred and up to two thousand watts.
They are installed in many industrial lasers for materials processing techniques, the latter spanning from plastic marking to sheet metal cutting, named in the order of increasing required power density delivered to the work piece. Other emerging processing techniques include high-precision micro-fabrication and additive metal printing. Industrial lasers can emit powers of the 100 kW-class and depend on high-power diode lasers (HPDL) — such as the herein studied high-power laser bars — as a key component. This workhorse of industrial laser technology is typically designed from broad-area lasers (BAL) and excels as the most efficient device to convert electrical into optical power. The emission of HPDLs is either routed directly to the processing site ("direct diode") [Ried18] or used to pump fiber and solid-state lasers, such as disk lasers [McD20]. Owing to the comparably poor beam quality (low brightness) of HPDLs, direct applications are limited to those requiring lower power density, e.g. hardening and marking, although consistent performance improvements increasingly enable their usage for even welding and brazing. Fiber

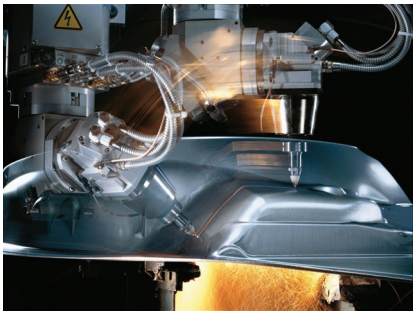

Figure 1.1: Laser-based metal cutting of a car body component ©TRUMPF Group

and solid-state lasers, on the other hand, offer higher brightness and are thus capable of, for instance, sheet metal cutting and deep-penetration welding. Here, HPDLs pump the used gain medium (e.g. Yb-doped fiber or crystal, respectively) at one of its absorption maxima and so provide the gain required for lasing. In effect, fiber and solid-state lasers enhance the input brightness of HPDLs, e.g. by a factor $> 20,000\times$ in a state-of-the-art fiber laser [Kan18]. Improvements in HPDL brightness generally allow further scaling in output power from the pumped lasers and bettered overall efficiency.
High-power laser bars – the matter of this dissertation – benefit from the advantages of their individual broad-area lasers, such as high conversion efficiency, but they also inherit their major drawback – the comparably poor beam quality. What is worse, bars were found to provide inferior beam quality in comparison to equivalent single-emitter lasers operated at the same per-emitter-power [Cru17]. This may be a pure ensemble effect but additional causes seem likely and need to be identified in order to eventually find solutions for improved bar beam quality.
It is thus at the heart of this thesis to study which physical mechanisms limit and which design optimizations enhance the performance of high-power diode-laser bars. In doing so, this work represents a contribution to the global optimization and design efforts that have allowed the brightness of HPDLs to increase by a factor of ten every eight years for the last 35 years [Kan18].
The remainder of this chapter firstly assesses the global laser market to showcase the economic relevance of the field, then analyzes the state of the art by comparing benchmark lasers, and finally outlines the structure of this thesis.

1.1. The global laser market

The world-wide laser market is predicted to amount to nearly $17 billion in 2020 revenue, reached by a steady annual growth of on average 12% p.a. since 2015, cf. Fig. 1.2(a). Exceptional growth rates of nearly 20% were observed in 2016 and 2017. About 42% of the lasers sold use diode technology as the core component while the remaining portion in many cases makes use of diode lasers as an auxiliary device, e.g. as pump laser. Grouped into market segments, about $6 billion were spent in 2019 on lasers for materials processing and lithography applications. This constitutes the largest market share of 40%, followed by the communications and optical storage sector (27%), cf. Fig. 1.2(b). The industrial lasers sold in the dominating market segment serve as tools for a variety of materials processing techniques, whose relative frequency is illustrated in Figure 1.2(c), and of which cutting (35%) is the by far the most important one. Three further applications, namely welding/brazing, marking, and semiconductor/display show similar shares of each

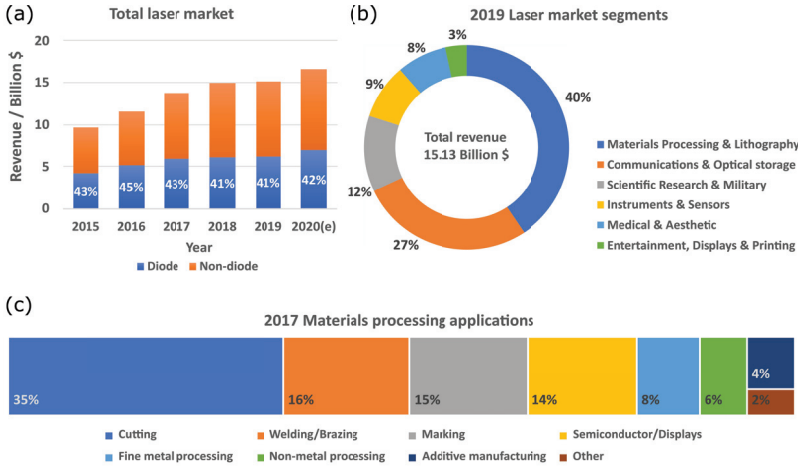

Figure 1.2: Metrics of the global laser market. (a) Annual revenue of the total laser market split into diode and non-diode contributions. (b) Market segment shares of the 2019 laser sales. (c) Applications of lasers sold in the materials processing segment in 2017. Data taken from [Hol18a] and [Gef20].

about 15%.

1.2. State of the art

The following firstly gives an overview of current industrial laser systems along with their specifications and secondly reviews recent notable publications on high-power laser bar performance.

Which materials processing technique a laser system is suitable for is determined by the emitted power P and the corresponding beam quality, quantified for instance via the *beam parameter product* BPP as introduced in Section 2.2. Combined, the *linear brightness* $B_{\mathrm{lin}} = P/\mathrm{BPP}$ expresses the power density of the emitted beam and it is among the most important parameters to characterize a beam. Table 1.1 lists commercial laser systems with top performance from a variety of vendors. They are based on four different technologies, namely fiber, disk, CO_2, and direct-diode lasers, of which disk and many direct-diode lasers incorporate high-power laser bars. The highest linear brightness B_{lin} is provided by fiber lasers with values up to 5.3 W/mm mrad, enabled by near-diffraction-limited beam quality BPP = 0.38 mm mrad, and are thus suitable for the most demanding

B_{lin} [#]	P / kW	BPP [†]	η / %	λ / nm	Type	Vendor / Product
5.3	2	0.38	32	1075	fiber	Trumpf TruFiber 2000
3.5	60	17	45	1070	fiber	IPG YLS-60000
3.0	12	4.0	37	1030	disk	Trumpf TruDisk 12001
2.3	8	3.5	8	1060	CO_2	Coherent DC 080
1.6	10	6.4	9	1060	CO_2	Trumpf TruFlow 10000
0.28	11	40	35	900-1080	direct DL	Laserline LDF series
0.15	4.5	30	40	920-970	direct DL	Trumpf TruDiode 4506
0.15	1.5	10	33	976	direct DL	IPG DLR-976-1500
0.13	4	30	31	900-1100	direct DL	Coherent HL DL4000HQ

Table 1.1: Commercial laser systems for high-power material processing applications ranked with descending brightness (product with highest available brightness selected per vendor and type), units [#] kW / mm mrad, [†] mm mrad. Specifications taken from vendors' online product catalogs as of January 2021, private communication with vendor, and [Ried18].

Publication	Year	P / kW	η / %	Operation	T / °C	FF / %	L / mm
[Sch07]	2007	1.1[#]	34	QCW	15	44	4
[Li08]	2008	1.0	56	CW	8	83	5
[Kna11]	2011	0.94	55	CW	20	77	5
[Fre15]	2015	1.98	57	QCW	-73	69	4
[Fre16]	2016	1.0	70	QCW	-70	69	4
[McD20]	2020	0.24[§]	59	CW	29	60	4
This work	2020	1.0	66	QCW	25	87	4
[Cru21]	2021	0.8	61	CW	15	87	4

Table 1.2: Notable publications on kW-class cm-bars, here focusing on emitted power P, the efficiency η at this operation point, and the used heat sink temperature T. All bars emit at 940 nm, except [#]at 980 nm. [§]state of the art in large-scale high-reliability production frame

processing applications. Disk lasers, here one using a Yb:YAG gain medium pumped by high-power laser bars, show brightness values as high as 3 W/mm mrad. The CO_2 laser is a mature technology that is steadily being replaced by the competing technologies not only due to its poor conversion efficiency. Direct-diode lasers excel in reduced system complexity as no optical to optical conversion step is required and make use of wavelength and polarization multiplexing for power scaling. Their brightness still falls behind the competing platforms which is due to their comparably poor beam quality with a BPP = 40 mm mrad in case of the highest brightness product listed here (0.28 W/mm mrad).

The object of study in this thesis is the 1 cm-wide high-power broad-area laser bar. Industrial large-scale fabrication with high reliability reaches power levels of [200:300] W as published in, for instance, [McD20] where 240 W-emitting bars for pump applications

Publication	Year	P / kW	$\Theta_{\mathrm{l,\,95\%}}$ / °	η / %	R_{th} / $\mathrm{KW^{-1}}$	Operation	T / °C	FF / %
[An15]	2015	0.29	8.3	58	0.21	CW	25	50
[Hei18]	2018	0.27	8.5	54	0.24	CW	29	60
[Str18]	2018	0.65	10.8	64	0.054	CW	15	70
This work	2020	1.0	8.8	61	0.02	QCW	25	69
This work	2020	1.0	10.8	54	0.05	QCW	25	69

Table 1.3: Notable publications on kW-class cm-bars, here focusing on emitted power P and lateral divergence angle $\Theta_{\mathrm{l,\,95\%}}$ at this operation point. All bars emit at 940 nm.

are presented. In an effort to minimize the cost per emitted power (from $<$ \$2 /W in aforementioned publication) ever increasing operation points have been targeted with 1 kW per bar as a landmark. The first demonstration that has reached this power level was published in 2007 and made use of a 4 mm-long resonator and 44% fill-factor (FF, that is the fraction of bar width occupied by active emitters) [Sch07]. The bar was driven in quasi-continuous wave (QCW) mode with an efficiency of 35%, cf. Tab. 1.2. After this milestone had been reached, the conversion efficiency needed to be improved, which suffered from the high series resistance $R_{\mathrm{s}} = 1.3\,\mathrm{m\Omega}$. One year later, the first continuous wave (CW) 1 kW-demonstration was reported with increased 83% FF and 5 mm cavity length [Li08] using high-heat-removal-capacity packages with a low thermal resistance $R_{\mathrm{th}} = 0.08\,\mathrm{K/W}$. From thereon more and more prototypes for this power level were developed. Another milestone in kW-class bar research was achieved at cryogenic temperatures $-73°\mathrm{C}$ enabling nearly 2 kW emitted power [Fre15], with record 70% efficiency at 1 kW [Fre16]. This thesis focuses on "room-temperature" operation as an industrial boundary condition instead and its design studies have let the 1 kW-efficiency increase to 66% in QCW-mode [Kar20]. Recent activities in which bars developed within this work were mounted in low-thermal-resistance packages reached 61% at 0.8 kW in CW mode [Cru21].

Aside from the desire for ever higher conversion efficiency, the beam quality of the emitted light also determines the merit of a bar design. An overview of notable publications on this matter is given in Table 1.3. Industry developments feed about 300 W in a lateral angle $\Theta_{\mathrm{l,\,95\%}}$ of about 8.5° in CW mode [An15, Hei18]. The heating in the devices has been identified as a major determinant of the lateral divergence, as will be elaborated on in Section 2.2, and it is quantified via the thermal resistance R_{th}, also listed in the table. An industrial prototype increased the emitted power to 0.65 kW at a divergence of 10.8°, also tested in CW mode but using high-capacity coolers with low thermal resistance $R_{\mathrm{th}} = 0.054\,\mathrm{K/W}$ [Str18]. Developments in the frame of this work allowed feeding 1 kW into an angle of 8.8° in QCW mode (using $R_{\mathrm{th}} = 0.02\,\mathrm{K/W}$) [Kar20].

1.3. Structure of this work

This thesis aims to study which physical mechanisms affect and which technological approaches improve the performance of 1 kW-emitting broad-area laser bars, whereby the focus is laid on the conversion efficiency η and the lateral divergence angle $\Theta_{\mathrm{l,\,95\%}}$ at the operation point.
In doing so, Chapter 2 provides the theoretical base of this work by firstly describing the design and working principle of broad-area laser bars and their comprising component — broad-area lasers (BAL). The work then summarizes what has been found to this date about the mechanisms governing the beam quality of BALs and thus provides insight on which design studies and the use of which technologies appear worthwhile for performance progression. Chapter 3 outlines the fabrication steps of the devices processed for this work and then details the characterization techniques and setups with a focus on the emitter-resolved beam-quality test station conceived and realized in the course of this thesis. The experimental results are divided into design studies seeking to increase the conversion efficiency, cf. Chapter 4, and those to lower the lateral divergence, cf. Chapter 5, while building on the findings from Chapter 4. Conclusions on the physical insights gained and the performance progresses achieved are complemented by a prospect to this work in Chapter 6.

2. Theoretical Background

This chapter lays the theoretical basis of this work. While it does not aim to span across all topics associated with diode-laser bars or to provide a comprehensive treatment, it shall highlight important equations and name relevant sources for further study.

2.1. Concept and physics of broad-area laser bars

Diode-laser bars are comprised of several individual diode lasers (emitters) processed onto one macroscopic chip of semiconductor material, cf. Fig. 2.1. The resultant incoherent superposition of these emitter's radiation aims to upscale the emission power per device. At the same time, this monolithic integration of several light sources reduces manufacturing costs (in $/W-optical-power) and shrinks total device footprint as compared to individually manufactured single-emitter lasers. The operation voltage for the latter and for bars of the same emitter type are comparable as the individual bar emitters are circuited in parallel. A common quantity used to characterize bar designs is the (lateral) fill-factor (FF). It reflects the fraction of the total bar width (of the distance between the edges of the two outmost emitters, to be exact: "the aperture") that is comprised of active emitters. For a number n_e of w-wide stripes with a spacing d_s in-between adjacent emitters[1] the FF reads

$$\mathrm{FF} = \frac{n_\mathrm{e} w}{w_\mathrm{aperture}} = \frac{n_\mathrm{e} w}{(w + d_\mathrm{s})(n_\mathrm{e} - 1) + w}.$$

The basic operation principle and the underlying physics does not differ between laser bars and single-emitter diode laser.
A plethora of literature covering semiconductor devices and diode lasers in particular is available. A few introductory books shall be mentioned for different foci of interest. [Sze07] treats a wide range of semiconductor devices as well as essential building blocks and several opto-electronic devices and may thus be a suitable starting point. A focus on the physics of diode lasers is laid on in [Col95] and [Chu12] deriving essential underlying equations, while [Epp13] is rather engineering-oriented and considers real-world laser designs and their design parameters. Diode lasers for high-power applications are covered by [Die00], also including chapters on fabrication, and by [Bac07] further detailing packaging and beam-combining systems.

Diode-laser bars for high-power applications typically make use of broad-area lasers (BAL) which are of the edge-emitting type. This is, a Fabry-Pérot resonator is formed by two facets cleaved perpendicular to the epitaxial growth direction (longitudinal modal

[1] The quantity pitch p is often used in literature and can be computed via $p = w + d_\mathrm{s}$.

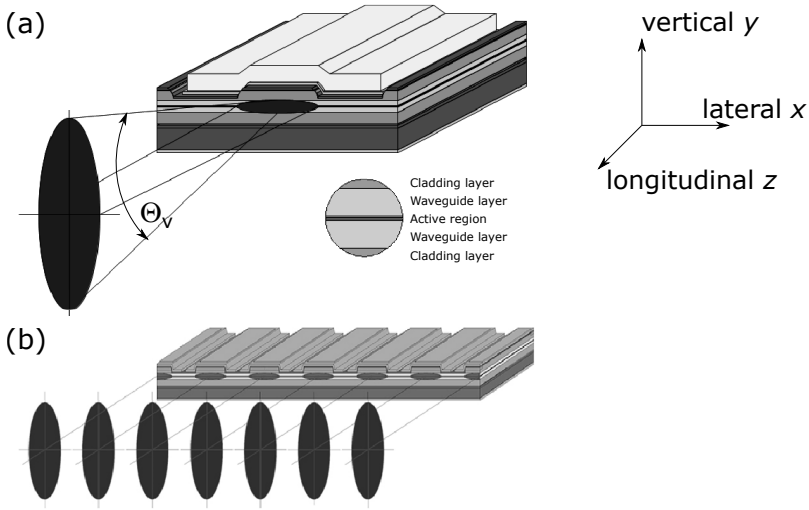

Figure 2.1: Illustration of broad-area lasers (BAL) in the further used coordinate system (a) Single-emitter laser with exemplary emission pattern (b) Laser bar comprised of several emitters processed on-chip. Not to scale, taken from [Erb00] ©Springer-Verlag

confinement). The resonator measures typically $1\,\text{mm} \leq L \leq 6\,\text{mm}$ in length and the laser light is extracted through of the facets exhibiting low reflectivity $R_\text{f} \leq 10\%$. Pumping is realized via charge carrier injection through a lateral-longitudinal current-path cross-section of width w, i.e. the stripe width, and is facilitated by a p-i-n-junction doping profile subject to forward bias. In case of BALs, w measures orders of magnitude above the emission wavelength $w \gg \lambda$ with typical values $50\ \mu\text{m} \leq w \leq 200\ \mu\text{m}$. Vertical confinement is nowadays realized via SCH-designs (seperate confinement heterostructure) as opposed to earlier double-heterostructure devices, expressing that modal and charge carrier confinement are realized by individually acting layer sequences. For emission in the 9xx nm-range, as targeted herein, the vertical waveguide is commonly grown from the $\text{Al}_x\text{Ga}_{1-x}\text{As}$ semiconductor compound whereby core and cladding layers (refractive index profile formed via molar fraction x and layer thicknesses) shape the vertical mode such that the desired mode width, position, confinement factor Γ and overlap with doped regions (one contributor to the internal loss α_i) is realized. Charge carrier confinement to reach the high carrier densities necessary for stimulated emission is commonly realized via strained $\text{In}_x\text{Ga}_{1-x}\text{As}$ quantum wells offering high material gain g_0 due to their narrow

charge-carrier energy distribution. The incorporated strain and the resultant energetic separation of heavy- and light-hole band further facilitate polarized emission; in the given case of compressive in-plane strain being of the transverse-electric (TE) type.
The mathematical description of the emission and recombination processes inside a laser diode [Col95, Chu12] find the threshold current I_{th} as

$$I_{\mathrm{th}} = wLj_{\mathrm{tr}} \cdot \exp\left(\frac{\alpha_{\mathrm{i}} + \alpha_{\mathrm{m}}}{\Gamma g_0}\right), \qquad \alpha_{\mathrm{m}} = -\frac{1}{2L}\ln\left(R_{\mathrm{f}}R_{\mathrm{r}}\right), \tag{2.1}$$

with the transparency current density j_{tr}, the mirror loss α_{m}, and the front and rear facet reflectivity values R_{f} and R_{r}, respectively. The emitted power P above threshold reads

$$P = \frac{hc}{e\lambda} \cdot \frac{\eta_{\mathrm{i}}}{1 + \alpha_{\mathrm{i}}/\alpha_{\mathrm{m}}} \cdot (I - I_{\mathrm{th}}),$$

with η_{i} the internal efficiency — characterizing the laser material — as the fraction of charge carriers that undergo stimulated recombination, as well as Planck's constant h, c the vacuum speed of light, and e the elementary charge. The slope efficiency S is defined as the derivative of the emission power

$$S = \frac{\mathrm{d}P}{\mathrm{d}I} = \frac{hc}{e\lambda} \cdot \frac{\eta_{\mathrm{i}}}{1 + \alpha_{\mathrm{i}}/\alpha_{\mathrm{m}}} \tag{2.2}$$

and reflects, reduced to the differential efficiency η_{d},

$$\eta_{\mathrm{d}} = \frac{\eta_{\mathrm{i}}}{1 + \alpha_{\mathrm{i}}/\alpha_{\mathrm{m}}},$$

the fraction of injected charge carriers above threshold that are converted to and emitted as lasing photons. The $I - V$ characteristic of diodes can be approximated to first order using

$$V(I) = V_0 + R_{\mathrm{s}} \cdot I,$$

with V_0 the voltage offset required to reach flatband conditions and R_{s} the equivalent series resistance the charge carriers experience whilst drifting and diffusing through the laser structure. From the equations above, the electrical-to-optical conversion efficiency η is derived as

$$\eta = \frac{P}{IV} = \eta_{\mathrm{i}} \cdot \frac{1}{1 + \alpha_{\mathrm{i}}/\alpha_{\mathrm{m}}} \cdot \frac{hc}{e\lambda(V_0 + R_{\mathrm{s}}I)} \cdot (1 - I_{\mathrm{th}}/I).$$

This gives a first impression on how to improve the conversion efficiency of a certain laser structure. While a high value η_{i} is required, α_{i}, R_{s}, and I_{th} need to be minimized. The particularity of this are the mutual dependencies between the parameters which compli-

cate efforts for efficiency improvements.
Non-radiative recombination processes, such as Shockley-Read-Hall and Auger recombination, as well as thermalization processes at band structure discontinuities or upon free-carrier-absorption heat up the structure. The dissipated power P_{diss} can be expressed as a function of the electro-optical efficiency η and the optical power P. Heat removal via a cooling architecture with the thermal resistance $R_{\mathrm{th}} = \mathrm{d}T/\mathrm{d}P_{\mathrm{diss}}$ allows the device to heat up by the temperature increase[2] ΔT_{AZ}.

$$P_{\mathrm{diss}} = IV - P = (1/\eta - 1)P \quad \Rightarrow \quad \Delta T_{\mathrm{AZ}} = R_{\mathrm{th}}(1/\eta - 1)P \tag{2.3}$$

The heating itself has manifold implications on the laser performance which essentially can be traced back to a change in lattice constants (and the corresponding band diagram, i.e. band gap energy E_{g} and refractive index n_{r}) and altered, Fermi-Dirac-determined, occupation of the latter. This affects, for instance, the gain distribution, the waveguide action, the carrier transport, and the relative strength of the different recombination channels. A simple but useful and commonly applied way of quantifying the impact of temperature changes onto laser performance defines the phenomenological characteristic temperatures T_0 and T_1, which describe the changes in threshold current and slope efficiency, respectively.

$$I_{\mathrm{th}}(\Delta T) = I_{\mathrm{th},0} \cdot \exp(\Delta T/T_0), \qquad S(\Delta T) = S_0 \cdot \exp(-\Delta T/T_1) \tag{2.4}$$

Here, $I_{\mathrm{th},0}$ and S_0 denote the values from Eqs. 2.1 and 2.2 at a chosen baseline temperature. While the threshold increases with temperature, the slope efficiency decreases.

2.2. Definition and governing effects of beam quality in broad-area lasers

The suitability of BALs for specific applications, such as material processing or laser pumping, crucially depends on the power density one can reach when focusing the emitted light. This focusability is a fundamental property of a laser beam and is commonly referred to as its beam quality. It cannot be improved via beam shaping optics and is, in the best case of diffraction-limited optical elements, conserved upon propagation along an optical path. This is why efforts to reach high power density need to start right at the light sources and their emission process.
A widespread way to quantify beam quality is the use of the *beam parameter product* BPP that is composed of the beam width w_0 at its smallest extent (beam waist) and its full

[2] Here referring to the temperature of the active zone (AZ) as a crucial determinant of laser performance, e.g. via its provided gain distribution.